



## NONLINEAR CYCLIC CHARACTERISTICS OF SOILS

Fred (Feng) Yi<sup>1</sup>

<sup>1</sup> Senior Geotechnical Engineer, C.H.J. Incorporated, 1355 E. Cooley Dr., Colton, CA 92324; E-mail: [fyi@chjinc.com](mailto:fyi@chjinc.com)

**Abstract:** For this paper, research on nonlinear cyclic characteristics of soils was reviewed. A new model is presented consisting of a modified equation for an initial loading curve and a modified equation for constructing the hysteresis loop. The performance of the model was evaluated by simulating the frequently utilized relationships of shear modulus versus shear strain and damping ratio versus shear strain of various types of soils accumulated over the past decades. The outcomes indicated that the new model presented describes the measured relationships with excellent correlations. The new model can simulate not only the work-hardening, but also work-softening behaviors of soils.

### INTRODUCTION

Since the late 1980's, several unusually large earthquakes have occurred throughout the world. Those earthquakes not only destroyed innumerable houses, buildings and other structures such as bridges but also devastated the lives of thousands of people. In particular, after the Great Hanshin Earthquake, the previously accepted concept that the magnitude of displacement caused by an earthquake will be centimeters or decimeters was totally changed by the fact that measured displacements were on the order of meters. The lessons learned from those disasters require geotechnical earthquake engineers to make more accurate predictions of the behaviors of soil structures under large earthquake excitation.

On the other hand, the dramatic development of semiconductor technology since the late 1980's has allowed the personal computer to become an indispensable tool for geotechnical engineers. More and more numerical analyses, such as two and three dimensional linear and nonlinear stress and deformation analyses, are now performed on personal computers. Until relatively recently, such numerical analyses would have cost a great amount of money or, in many cases, would have been impossible.

Although hardware capable of satisfying the calculation demands of geotechnical engineers is readily available, crucial technology to model the seismic behavior of soils has not kept pace, and, in fact, has fallen far behind. In this paper, a new constitutive model simulating cyclic characteristics of soils is proposed. It is intended not only to provide a better simulation of seismic behavior of soils but also to fully utilize the historical data accumulated during past decades.

### SIMULATION OF CYCLIC CHARACTERISTICS OF SOILS

Although elasto-plastic theory has been utilized to simulate the nonlinear

behavior of soils under cyclic loading in recent years, the most widely used models are still nonlinear type models. The nonlinear type models usually include two parts: (1) the initial loading stress-strain nonlinear curve, extended also into the negative domain, usually called a initial loading curve, skeleton curve or backbone curve, and (2) the constructed hysteresis loop described by subsequent unloading and reloading stress-strain curves. In this paper, the term “skeleton curve” will be used to refer to the initial loading curve, because it will represent the envelope of the stress-strain relationship in cases where stress degradation occurs. Although several skeleton curves have been proposed in the past (Kondner and Zelasko 1963; Hardin and Drnevich 1972; Matasović and Vucetic 1993; Nakagawa and Soga, 1995; Ni et Al. 1997), a rule first suggested by Masing (1926), known as “Masing’s Rule”, has been commonly utilized in most research to construct the stress-strain hysteresis loop. By utilizing Masing’s Rule, the nonlinear stress-strain relationships of soils under cyclic loading can be constructed as illustrated in Figure 1 (Ishihara, 1996).

Let the initial loading stress-strain curve be expressed by Eq. (1), with the extension in negative domain.

$$\tau = f(\gamma) \quad (1)$$

where  $\tau$  and  $\gamma$  represent shear stress and shear strain, respectively.

Masing’s Rule assumes that:

(1) the shear modulus on each loading reversal is equal to the initial tangent modulus for the initial loading curve; and (2) the unloading stress-strain relationship keeps the same shape as that of the initial loading curve in negative domain but is magnified by a factor of two, while the reloading stress-strain relationship has the same shape as that of the initial loading in the positive domain also magnified by a factor of two. Therefore, as shown in Figure 1, if loading reversal occurs at point  $A$  where shear strain is equal to  $\gamma_a$  and shear stress is equal to  $\tau_a$ , then the subsequent unloading from the reversal point  $A$  can be expressed by Eq. (2a).

$$(\tau - \tau_a) / 2 = f((\gamma - \gamma_a) / 2) \quad (2a)$$

If the unloading curve defined by Eq. (2a) reaches point  $B$  in the negative domain, the stress-strain curve is assumed to follow the initial loading curve further in the negative domain. If the reloading takes place at point  $B$ , the stress-strain curve for the reloading is given by an equation similar to Eq. (2a) in which the signs of  $\tau_a$  and  $\gamma_a$  are changed. That is:

$$(\tau + \tau_a) / 2 = f((\gamma + \gamma_a) / 2) \quad (2b)$$

If the initial loading curve is intersected again at point  $A$  during the reloading, further loading is assumed to following the initial loading curve in the positive domain. Similarly, if the initial loading curve is intersected again at point  $B$  during the unloading, further loading is assumed to following the initial loading curve in the negative domain. Pyke (1979) stated that this should be considered as a third rule

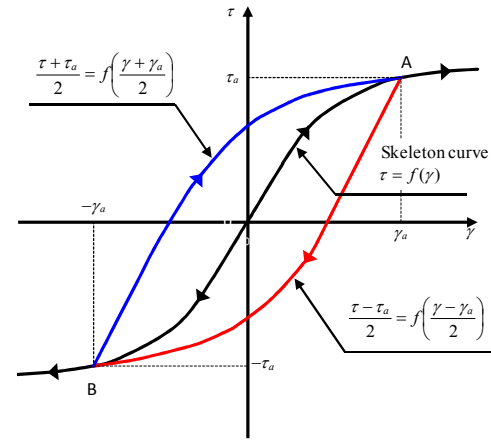


**Figure 1 Construction of unloading and reloading based on Masing’s Rule (Ishihara, 1982, 1996)**

added to the original Masing's Rule. In order to be applicable to irregular cyclic loadings, Pyke (1979) mentioned that a fourth rule should be also added to the three listed above, i.e., if the current loading or unloading curve intersects the curve described by a previous loading or unloading curve, the stress-strain curve follows that previous curve.

For such a constructed hysteresis loop (Figure 1), the area of the loop ( $\Delta W$ ) is the strain energy dissipated in the given unloading and reloading cycle. The strain energy of a linear material corresponding to the stress-strain level ( $\tau_a, \gamma_a$ ) is defined as:

$$W = \frac{1}{2} f(\gamma_a) \gamma_a \quad (3)$$

The damping characteristics of the soil (represented by the damping ratio,  $D$ ), is defined as:

$$D = \frac{1}{4\pi} \frac{\Delta W}{W} \quad (4)$$

Ishihara's (1982) research indicated that by applying Masing's Rule to hyperbolic type initial loading curves, the damping ratio defined by Eq. (4) can be computed as:

$$D = \frac{2}{\pi} \left( \frac{2 \int_0^{\gamma_a} f(\gamma) d\gamma}{f(\gamma_a) \gamma_a} - 1 \right) \quad (5)$$

The initial loading curves are customary expressed by either hyperbolic type (Kondner and Zelasko 1963; Hardin and Drnevich 1972) or Ramberg-Osgood type (Ramberg and Osgood 1943; Richart 1975; Hara 1980) models. As the stress is an implicit function of strain in Ramberg-Osgood type models, hyperbolic type models are more often used in practice.

Of hyperbolic type models, the most famous and most widely used model is the one initially proposed by Kondner and Zelasko (1963) (referred to as KZ model hereafter) and lately redefined by Hardin and Drnevich (1972b). Kondner and Zelasko (1963) formulated the stress-strain relationship for skeleton curves by the hyperbolic equation as follows,

$$\tau = \frac{G_0 \gamma}{1 + (G_0 / \tau_{ult}) \gamma} \quad (6)$$

where  $G_0$  is the initial tangent shear modulus at  $\gamma \rightarrow 0$  and  $\tau_{ult}$  is the shear stress when  $\gamma \rightarrow \infty$  and is usually called shear strength.

For the KZ model defined in Eq. (6), Ishihara (1982) found that the calculated damping ratio converges to  $2/\pi=0.637$ . This value is much higher than the measured maximum value of the damping ratio that usually ranges from 0.2 to 0.4. He pointed out that the KZ model is incapable of describing the soil stress-strain behavior with the desired degree of accuracy.

Several individuals proposed modifications to the KZ model (Matasović and Vucetic 1993; Nakagawa and Soga 1995; Ni et al. 1997). Matasovic and Vucetic (1993) studied the behavior of fully saturated liquefiable sands under undrained cyclic loading and proposed a modified Kondner and Zelasko model (abbreviated as MKZ). In the MKZ model, the initial loading curve was expressed in a normalized form with respect to the vertical effective consolidation stress,  $\sigma'_{vc}$ .

$$\tau^* = f^*(\gamma) = \frac{G_{m0}^* \gamma}{1 + \beta_0 \left( (G_{m0}^* / \tau_{m0}^*) |\gamma| \right)^s} \quad (7a)$$

where  $\tau^* = \tau / \sigma'_{vc}$ ,  $\tau_{m0}^* = \tau_{m0} / \sigma'_{vc}$ , and  $G_{m0}^* = G_{m0} / \sigma'_{vc}$ .  $G_{m0}$  is the initial tangent shear modulus at time  $t=0$ ,  $G_{m0} = G_0 \cdot \tau_{m0}$  is the shear strength of the soil. The curve-fitting constants  $\beta_0$  and  $s$  adjust the position of the curve along the ordinate and control the curvature.

During the second and subsequent cycles, the stress-strain behavior was characterized by the degrading backbone curves that were defined as,

$$\tau^* = f^*(\gamma) = \frac{G_{mt}^* \gamma}{1 + \beta_0 \left( (G_{mt}^* / \tau_{mt}^*) |\gamma| \right)^s} \quad (7b)$$

where,  $G_{mt}^* = G_{m0}^* \sqrt{1-u^*}$ ,  $\tau_{mt}^* = \tau_{m0}^* (1-u^*)$ , and  $u^* = u / \sigma'_{vc}$ .  $u$  is the residual excess pore-water pressure. Eq. (7b) represents a series of degraded stress-strain curves in the subsequent cycles due to the increase of residual excess pore-water pressure. This model significantly increases the accuracy in simulating each hysteresis loop. However it is uncertain in the application that, if the previous maximum shear strain is exceeded, which backbone curve the unloading and reloading curves should follow.

By studying cyclic torsional shear test results, Nakagawa and Soga (1995) suggested a new relationship between the shear modulus ratio and shear strain as:

$$\frac{G}{G_0} = \frac{1}{1 + \alpha_1 |\gamma|^{\beta_1}} \quad (8)$$

where  $\alpha_1$  and  $\beta_1$  are material constants defining the nonlinearity of a skeleton stress-strain curve. This relationship produces a much better curve fitting with the measured data. However, the coupling relationship between  $\alpha_1$  and  $\beta_1$  creates some uncertainty with respect to the parameters since not all of the measured data exist in linear relationships within a double-logarithmic plot as indicated in their paper.

Ni, et al (1997) proposed the modified initial loading curve as:

$$\tau = \frac{G_0 \gamma}{1 + |\gamma / \gamma_r|^{\beta_2}} \quad (9)$$

in which  $\beta_2$  is a constant and  $\gamma_r$  is the reference strain defined by Hardin and Drnevich (1972b) as the ratio of shear strength and initial shear modulus.

$$\gamma_r = \tau_{ult} / G_0 \quad (10)$$

It is noted that Eq. (9) will become the original KZ model if  $\beta_2$  is set to unity. Although some calculated  $G/G_0 \sim \gamma$  relationships were given in their paper, no calculated stress-strain relationships were reported. In fact, this model produces a much higher shear stress at a reasonable range of failure shear strain, say 0.01 to 0.1. For example, even for the data used in their research, the calculated shear stress at a shear strain level of 0.01 is as high as 2.2 times the shear strength, while it becomes 4.6 times the shear strength at a strain level of 0.1.

Although it was noticed two decades ago that the application of the Masing's Rule would result in an overestimate of the damping ratio (Ishihara, 1982), little research can be found to refine this effect. Pyke (1979) proposed a modification to the second rule of Masing's Rules. Instead of a factor of two, Pyke (1979) suggested a factor  $c$  where

$$c = \left| \pm 1 - \tau_a / \tau_{ult} \right| \quad (11)$$

in which the first term is negative for unloading and positive for reloading. Thus, the scale will normally be changed by a factor of less than two. Although, Pyke did not mention the effect of his modification on the damping ratio, it is not difficult to find that the damping ratio will converge to value given by the traditional Masing's Rule when  $\tau_a \rightarrow \tau_{ult}$ .

Wakai et al. (2001) are among the few researchers trying to solve the problem. Instead of Masing's Rule, they suggested Eq. (12) for the unloading and reloading curves.

$$\tilde{\tau} = \frac{a\tilde{\gamma}^n + G_0\tilde{\gamma}}{1 + b\tilde{\gamma}} \quad (12)$$

where  $G_0$ ,  $b$  and  $n$  are constants and  $a$  is dependent on other parameters, while  $\tilde{\tau}$  and  $\tilde{\gamma}$  represent the parallel translated stress-strain coordinate.

$$\tilde{\tau} = |\tau - \tau_a| \quad \text{and} \quad \tilde{\gamma} = |\gamma - \gamma_a| \quad (13)$$

The contribution of Wakai et al. is the introduction of a hysteresis loop function rather than scaling the initial loading curve. However, because the parameters are unclear and hard to determine, the application of this model is difficult. Also, they utilized the same equation as that of the KZ model for the initial loading curve. This results in limitations in simulating the measured stress-strain relationships.

## PROPOSED CYCLIC STRESS STRAIN MODEL OF SOILS

By examining the KZ model in detail, it is not difficult to notice that the stress-strain relationship is fully controlled by initial shear modulus and shear strength. For this reason, it is also called a two parameter model. As pointed out by Ishihara (1982), in some cases it is difficult to specify both the strain dependent shear modulus and damping ratio by using only two parameters. Particularly, the strain-dependent damping ratio is automatically determined once the abovementioned two parameters are given. In fact, the measured data indicated that stress-strain curves might be above or below the curve obtained from the KZ model in the range between small shear strain levels and shear strain levels near failure. Also the maximum value of the measured damping ratio is much smaller than that automatically determined by the KZ model and Masing's Rule.

The abovementioned drawback can be eliminated simply by introducing two additional parameters related to the shape of stress-strain curve and the damping ratio.

### *Skeleton curve*

Assume a stress-strain level near failure (for example, the maximum shear strain available from laboratory tests, usually ranged from 0.01 to 0.1) to be  $(\tau_f, \gamma_f)$ . The second shear modulus at this point can be expressed as  $G_f = \tau_f / \gamma_f$ . By normalizing Eq. (6) with respect to  $G_f$  and revising the equation, one obtains

$$\tau' = \frac{G_0\gamma'}{G_f + R_f G_0\gamma'} \quad (14)$$

where,  $\tau' = \tau / \tau_f$ ,  $\gamma' = \gamma / \gamma_f$ ,  $G_f = \tau_f / \gamma_f$ , and  $R_f = \tau_f / \tau_{ult}$ .

To better fit all of the test data, Eq. (14) can be modified by introducing a parameter,  $\alpha$ , as:

$$\tau' = \frac{G_0 \gamma'}{G_f + R_f G_0 |\gamma'|^\alpha} \quad (15)$$

or in form of original shear stress and shear strain,

$$\tau = \frac{G_0 \gamma}{1 + \frac{R_f}{1 - R_f} \left| \frac{\gamma}{\gamma_f} \right|^\alpha} \quad (16)$$

When expressed as shear modulus ratio, one obtains

$$\frac{G}{G_0} = \frac{1}{1 + \frac{R_f}{1 - R_f} \left| \frac{\gamma}{\gamma_f} \right|^\alpha} \quad (17)$$

where,

$$R_f = 1 - (G_f/G_0) \quad (18)$$

Eq. (18) is derived from shear strain level of  $\gamma = \gamma_f$ . At this strain level, Eq. (16) and Eq. (6) are identical. For practical use,  $\gamma_f$  can be taken as the maximum shear strain available from laboratory test data.

Note that the parameter,  $\alpha$ , controls the shape of initial loading curve in the range of shear strain between small values and large values near failure. When  $\alpha \leq 1$ , a work-hardening stress-strain curve is produced, while at values of  $\alpha > 1$ , a work-softened stress-strain curve is produced. This parameter,  $\alpha$ , is referred to as the *shape parameter of nonlinearity*. Figure 2 illustrates the effect of  $\alpha$  to the shape of stress-strain relationships.

### Unloading-reloading curves

Detailed research indicated that the fitness of the calculated to the measured data of the damping ratio is still beyond what is expected even when the initial loading curve is modified to Eq. (16), if the Masing's Rule is applied. This means that the assumption that the unloading and reloading curves have the same shape as the enlarged initial loading curve cannot properly represent the damping characteristics of soils under cyclic loading. To avoid the overestimation of the damping ratio, the shape of hysteresis loop for unloading and reloading must be modified.

Instead of scaling the initial loading curve to construct the unloading-reloading loop, a new function can be defined as follows:

$$\tau = \frac{G_0 \gamma}{1 + B \cdot \left| \gamma / \gamma_a \right|^\beta} \quad (19)$$

where,  $\beta$  is a parameter related to the damping ratio and

$$B = \frac{R_f}{1 - R_f} \left| \frac{\gamma_a}{\gamma_f} \right|^\alpha \quad (20)$$

$B$  is a constant within the loop of  $(\tau_a, \gamma_a)$ . Thus, the second rule of Masing's Rules can be modified as that the shape of the reloading curve is the same as the positive portion of Eq. (19) increased by a factor of two and the unloading curve has the same shape as the negative portion of Eq. (19) increased by a factor of two, i.e.,

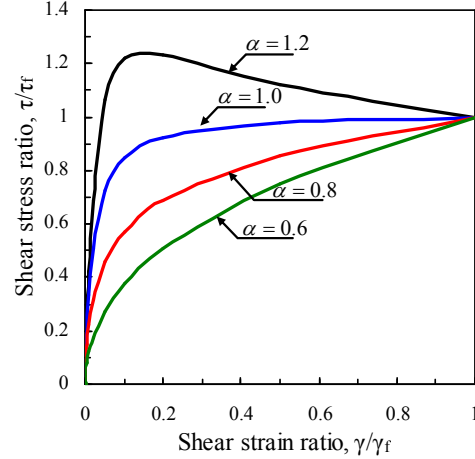


**Figure 2 Stress-strain curves with different  $\alpha$**

$$\frac{\tilde{\tau}' \mp 1}{2} = \frac{G_0(\tilde{\gamma}' \mp 1)/2}{G_a + B \cdot G_a |(\tilde{\gamma}' \mp 1)/2|^\beta} \quad (21)$$

where  $\tilde{\tau}' = \tau/\tau_a$ ,  $\tilde{\gamma}' = \gamma/\gamma_a$ ,  $G_a = \tau_a/\gamma_a$ . The negative sign is for unloading and the positive sign is for reloading. The stress and strain are normalized to those at the reversal point A (see Figure 3).

### Shape parameter of nonlinearity, $\alpha$

It is not difficult to calculate the *shape parameter of nonlinearity*,  $\alpha$ , based upon measured data between  $G/G_0$  and  $\gamma$ . In fact, Eq. 17 can be rewritten as:

$$\alpha \log\left(\frac{\gamma}{\gamma_f}\right) = \log\left[\left(\frac{1}{(G/G_0)} - 1\right) \frac{1 - R_f}{R_f}\right] \quad (22)$$

If the measured data between  $G/G_0$  and  $\gamma$  is known, this data can be re-plotted as in Figure 4. The *shape parameter of nonlinearity* can then be determined by regression analysis.

It has been noted that in some cases the measured data does not exist as a linear relationship between left and right terms of Eq. (22). To obtain a better fit to the measured data, it is suggested to plot the measured and calculated data on the same graph and to obtain a better fit by adjusting the value of  $\alpha$ . This can be easily done by utilizing spreadsheet software such as Excel.

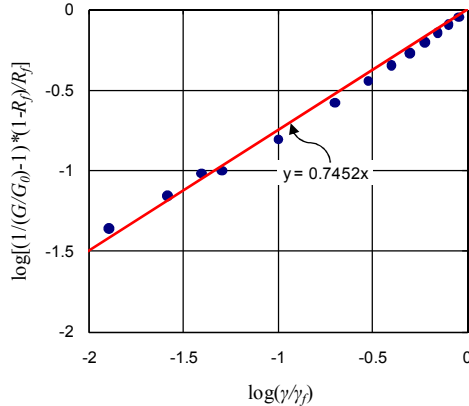


Figure 4 Determination of  $\alpha$

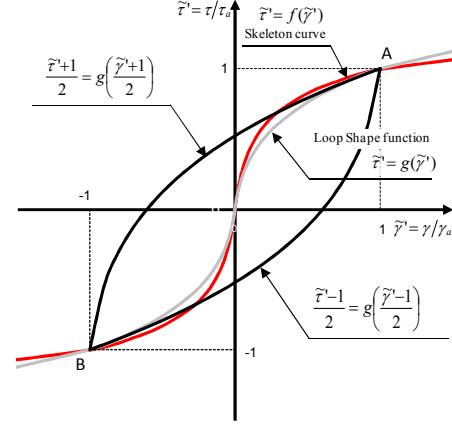


Figure 3 Construction of unloading and reloading curves

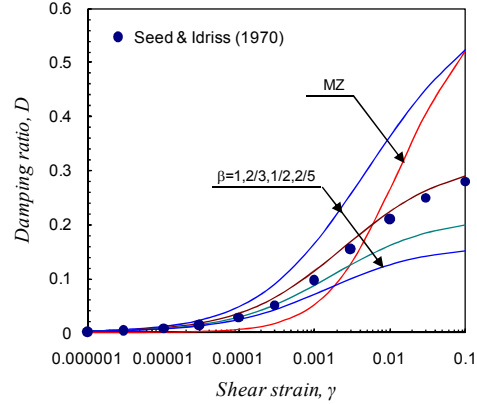


Figure 5 Effect of  $\beta$  on damping ratio

### Damping parameter, $\beta$

Compared to the *shape parameter of nonlinearity*,  $\alpha$ , the *damping parameter*,  $\beta$ , is more complicated to determine. By introducing Eq. (18) into Eq. (5), the damping ratio for the proposed model can be calculated by,

$$D = \frac{2}{\pi} \left[ 2(1+B) \int_0^1 \frac{\tilde{\gamma}'}{1+B\tilde{\gamma}'^\beta} d\tilde{\gamma}' - 1 \right] \quad (23)$$

Although for an arbitrary value of  $\beta$ , numerical integration is necessary to compute the damping ratio, the integration of Eq. (23) is possible at,

$$\beta = 2/(m+1) \quad (m=1, 2, 3, \dots) \quad (24)$$

By plotting  $D$  vs.  $\gamma$  relationships of different  $\beta$  together with measured data as in Figure 5, it is not difficult to evaluate the value of  $\beta$  with sufficient accuracy.

## EVALUATION OF MODEL PERFORMANCE

Matasović and Vucetic (1993) performed extensive testing on several types of liquefiable sands. The test results obtained from Santa Monica Beach (SMB) sand were simulated utilizing the proposed model. Figures 6 through 8 illustrate measured and simulated  $\tau$  vs.  $\gamma$ ,  $G/G_0$  vs.  $\gamma$ , and  $D$  vs.  $\gamma$  relationships, respectively. For comparison, results calculated based on the KZ and MKZ models are also illustrated. It can be seen that the proposed model generally agrees with the MKZ model and gives much better correlations with measured data than the KZ model.

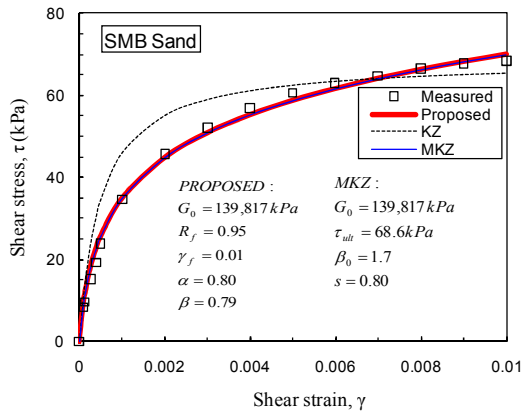


Figure 6 Simulation of  $\tau \sim \gamma$  relationship

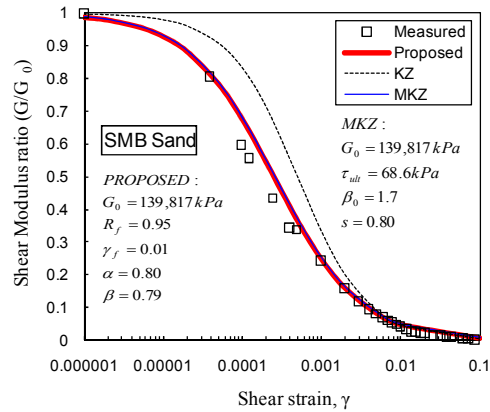


Figure 7 Simulation of  $G/G_0 \sim \gamma$  relationship

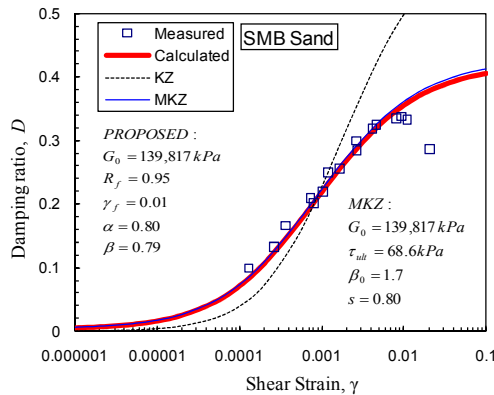


Figure 8 Simulation of damping ratio

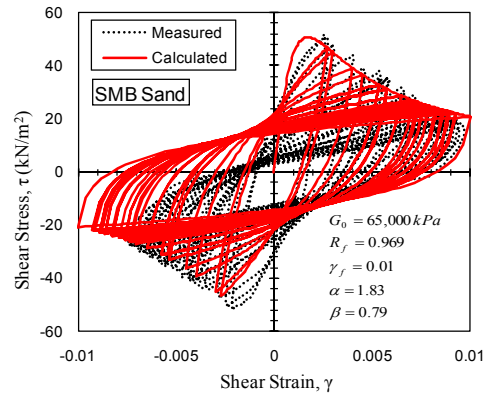


Figure 9 Simulation of hysteresis loop

One of the important aspects of the proposed model is the construction of the hysteresis loop between shear stress and shear strain. Figure 9 demonstrates the simulation of hysteresis loop for the data obtained by Matasović and Vucetic. Although, the asymmetric pattern occurring in the measured data was not fully reproduced, the results presented in Figure 9 indicate that the difference between the experimental and analytical curves is small, verifying that the proposed model is

applicable to liquefiable sands.

In fact, the asymmetric characteristics of liquefied sand can be appropriately simulated by adding conditions when programming. Details related to this modeling will be discussed in subsequent papers.

Although it seems that the proposed model needs one more parameter than the MKZ model ( $G_0, R_f, \gamma_f, \alpha$ , and  $\beta$  versus  $G_0, \tau_{ult}, \beta_0$ , and  $s$ ) to obtain the same results as shown in Figures 6 through 8, the MKZ model requires a fifth parameter,  $u$ , to simulate the degradation of the stress-strain relationship as shown in Figure 9. The calculation of  $u$  requires an excess pore water pressure model and an effective stress analysis program. By solely using these five parameters, the proposed model is able to simulate not only the liquefaction-induced degradation but also the work-softening behaviors of unsaturated soils.

## CONCLUSIONS

A survey of the reported literature related to hyperbolic models and Masing's Rule has been performed by this author. Based on that survey, a new model for the simulation of the cyclic characteristics of soils is proposed. The new model modifies not only the initial loading curve but also the equation for constructing the hysteresis loop. From the study performed by this author, the following conclusions about the modeling of the cyclic behavior of soils can be derived.

- 1) The initial loading curve of shear stress-strain relationships can be more accurately simulated by adding an additional *shape parameter of nonlinearity*,  $\alpha$ . With this modification, the new skeleton equation is able to model not only work-hardening conditions but also work-softening conditions.
- 2) The shape of hysteresis loop is not necessarily the same as that of the enlarged skeleton curve, but is in a different function. This function can be defined by introducing a *damping parameter*,  $\beta$ .
- 3) The new model can be used to directly simulate saturated liquefiable sand, even when the sand undergoes significant cyclic degradation.

The new model requires five parameters,  $G_0, R_f, \gamma_f, \alpha$ , and  $\beta$ . Calculation methods for obtaining all of these parameters are illustrated. This will assist in understanding the model and calculating the parameters from test results.

The new model was used to simulate  $G$  vs.  $\gamma$  and  $D$  vs.  $\gamma$  relationships most often utilized for various types of soils accumulated over the past decades and illustrated with adequate accuracy (the results will be published at later date). The parameters obtained can be directly utilized in the prediction of soil behavior under cyclic loading conditions, when measured data is not available.

The new model can be easily coupled within a time-domain program. Even for an equivalent linear method program, the new model is preferable in order to avoid interpretation of measured  $G$  vs.  $\gamma$  and  $D$  vs.  $\gamma$  data, since, in some instances, direct interpretation of measured data will result in stress-strain relationships which do not fit the actual condition being simulated.

Although the current model is a one dimensional model, it is possible to extend it into a model applicable to three dimensional stress spaces. This will be discussed at later date.

## ACKNOWLEDGMENTS

The author appreciates the support and help by Mr. Robert J. Johnson, PE, GE, and Mr. Allen D. Evans, PE, GE, in the preparation of this manuscript.

## REFERENCES

- Hara, A. (1980), "Dynamic deformation characteristics of soils and seismic response analysis of the ground," *Dissertation submitted to the University of Tokyo*, Tokyo, Japan
- Hardin, B.O. and Drnevich, V.P. (1972a). "Shear modulus and damping in soils: measurement and parameter Effects." *Proc. ASCE, Vol. 98, SM6*, 603-624
- Hardin, B.O. and Drnevich, V.P. (1972b). "Shear Modulus and Damping in Soils: Design Equation and Curves." *Proc. ASCE, Vol. 98, SM7*, 667-692
- Ishihara, K. (1982). "Evaluation of soil properties for use in earthquake response analysis." *International Symposium on Numerical Models in Geomechanics*, Zurich.
- Ishihara, K. (1996). "Soil behavior in earthquake geomechanics." Oxford Science Publication
- Kondner, R. L., and Zelasko, J. S. (1963). "A hyperbolic stress-strain formulation of sands." *Proc. 2<sup>nd</sup> Pan Am. Conf. on Soil Mech. And Found. Engrg., Brazilian Association of Soil Mechanics*, São Paulo, Brizil, 289-324
- Masing, G. (1926). "Eigenspannugen und Verfestigung beim Messing." *Proc. 2<sup>nd</sup> Int. Cong. On Appl. Mech.*, 332-335.
- Matasović, N. and Vucetic, M. (1993). "Cyclic characterization of liquefiable sands." *Journal of Geomechanical Engineering, Vol. 119, No. 11*, 1805-1822
- Nakagawa, K. and Soga, K. (1995). "Nonlinear cyclic stress-strain relations of soils." *Third International Conference on Recent Advances in Geotechnical Earthquake Engineering and Soil Dynamics*, St. Louis, April 2-7, 57-60
- Ni, Shean-Der, Siddharthan, Raj V. and Anderson, G. (1997). "Characteristics of Nonlinear Response of Deep Saturated Soil Deposits." *Bulletin of the Seismological Society of American, Vol. 87, No. 2*, 342-355.
- Pyke, R. (1979). "Nonlinear soil models for irregular cyclic loadings," *Journal of Geotechnical Engineering, ASCE, Vol. 105, No. GT6*, 715-726.
- Ramberg, W., and Osgood, W. R. (1943). "Description of stress-strain curves by three parameters." *NACA Tech. Note No. 902*, Washington, D.C.
- Richard, F.E., Jr., (1975). "Some effects of dynamic soil properties on soil-structure interaction." *Journal of Geotechnical Engineering, ASCE, Vol. 101, No. GT12*, 1193-1240.
- Seed, H.B. and Idriss, I.M. (1970). "Soil moduli and damping factors for dynamic response analyses," *Report No. EERC 70-10, Earthquake Engineering Research Center*, University of California, Berkeley.
- Wakai, A., Ugai, K., and Sato, M. (2001). "Finite element simulation for dynamic centrifuge test of a simple slope", *10th International Conference of the Association for Computer Methods and Advances in Geomechanics*, pp.989-992, Tucson AZ, USA